








COMMUNICATIONS PHYSICS

ARTICLE

<https://doi.org/10.1038/s42005-019-0157-1>

OPEN

Picosecond timescale tracking of pentacene triplet excitons with chemical sensitivity

R. Costantini ^{1,2}, R. Faber ³, A. Cossaro ¹, L. Floreano¹, A. Verdini ¹, C. Hättig⁴, A. Morgante ^{1,2}, S. Coriani ³ & M. Dell'Angela ¹

Singlet fission is a photophysical process in which an optically excited singlet exciton is converted into two triplet excitons. Singlet fission sensitized solar cells are expected to display a greatly enhanced power conversion efficiency compared to conventional single-junction cells, but the efficient design of such devices relies on the selection of materials capable of harvesting triplets generated in the fission chromophore. To this aim, the possibility of measuring triplet exciton dynamics with chemical selectivity paves the way for the rational design of complex heterojunctions, with optimized triplet conversion. Here we exploit the chemical sensitivity of X-ray absorption spectroscopy to track triplet exciton dynamics at the picosecond timescale in multilayer films of pentacene, the archetypal singlet fission material. We experimentally identify the signature of the triplet exciton in the Carbon K-edge absorption spectrum and measure its lifetime of about 300 ps. Our results are supported by state-of-the-art *ab initio* calculations.

¹CNR-IOM, Strada Statale 14 - km 163.5 in AREA Science Park, Basovizza, 34149 Trieste, Italy. ²Physics Department, University of Trieste, Via Valerio 2, 34127 Trieste, Italy. ³Department of Chemistry, Technical University of Denmark, Kemitorvet, Building 207, DK-2800 Kgs. Lyngby, Denmark.

⁴Arbeitsgruppe Quantenchemie, Ruhr-Universität Bochum, D-44780 Bochum, Germany. Correspondence and requests for materials should be addressed to S.C. (email: soco@kemi.dtu.dk) or to M.D'A. (email: dellangela@iom.cnr.it)

When absorbing high energy photons, conventional photovoltaic cells are affected by thermalization of charge carriers, which is the major channel of efficiency loss for solar energy conversion. Two possible strategies to overcome such losses are down-conversion and multiexciton generation^{1–3}, the latter one including the singlet fission (SF) process. The application of SF in solar energy conversion devices was demonstrated to raise the power conversion efficiency above the Shockley–Queisser limit⁴, and this fact made the study of SF gain a large popularity in solar energy research. Over the past few years, a lot of efforts have been made to design and characterize high-fission-yield chromophores, mainly acene derivatives^{5–9} and conjugated polymers^{10–12}, but an elaborate device architecture is required to take advantage of the carrier multiplication in these materials^{13,14}. The fission material should be coupled with both an electron and a hole acceptor, and proper energy level alignment and interface morphology are required to maximize triplet exciton harvesting while reducing the contribution from singlet excitons to the photocurrent, as this competing channel does not provide any extra gain to the power conversion efficiency. Amongst the fission chromophores, pentacene is to date the most studied one. The fission process is exothermic and unidirectional, because the relaxed triplet state of pentacene has less than half the energy of the singlet state^{9,15}. Pentacene triplet excitons, with lifetimes spanning from picoseconds up to nanoseconds, have already been measured in thick films by means of several optical spectroscopies, such as transient absorption¹⁶ and time resolved two-photon photoemission (tr-2PPE)¹⁷. However, the application of such powerful experimental techniques to complex architectures with more than one chromophore does not allow the disentanglement of the contribution from different excitation sites, due to the lack of chemical sensitivity. Recently, time resolved X-ray spectroscopies have been applied to the study of photoexcited states in molecules either in solution or in gas phase^{18,19}. Such techniques offer chemical selectivity since they probe excitations of localized core electrons to unoccupied valence states. The extension of these studies to the condensed phase, where SF takes place, is, however, very challenging due to the delicate balance between obtaining an acceptable pump-probe statistics and limiting the optical and X-ray induced sample damage.

In this study, we present a combined experimental and theoretical study of triplet dynamics in pentacene films, probed by time resolved picosecond carbon K-edge X-ray absorption spectroscopy (tr-XAS) at a synchrotron facility. Measurements of the electronic structure dynamics in the pico- and femtosecond timescales are nowadays routinely performed at pulsed X-ray sources like free electron lasers (FELs) and high harmonic generation (HHG) setups.^{20–23} However, if compared with FELs, the sample damage in the pump-probe scheme at the synchrotron is limited thanks to the low X-ray pulse energy at megahertz repetition rate and the use of optical pulses which best match the conditions in tr-2PPE. Moreover, at synchrotrons, the photon energy is easily tuned across the carbon K-edge in a continuous way. We present here evidence of pentacene triplet excitons in the X-ray absorption spectra, and we measure the triplet state lifetime, which is found to be in agreement with reference tr-2PPE measurements performed *in situ*. The identification of transitions in the XAS spectra attributed to molecules in the triplet state, is supported by *ab initio* calculations of the core-absorption spectra of both the ground state and the triplet-excited state at resolution-of-identity (RI-) second-order approximate coupled-cluster singles and doubles (CC2) level of theory. To the best of our knowledge, this is the first extension of RI-CC2 to the calculation of core spectra (both excitation energies and intensities) of triplet excited states.

Results

Characterization of the pentacene film. The molecular films have been deposited *in situ* in the ultra-high vacuum (UHV) experimental chamber to ensure the best molecular ordering and prevent contamination. We have studied pentacene films deposited on a fullerene (C₆₀) covered Ag(111) substrate. The C₆₀ buffer layer drives pentacene standing-up orientation and ordering into a bulk-like crystalline phase²⁴, whose herringbone molecular pairing strongly favours the SF process, as compared with other possible packing structures. Details on film growth and thickness evaluation are reported in the Methods section and in the Supplementary Note 1. We underline that we prepared pentacene films thick enough so that our tr-XAS measurements are sensitive only to the electron dynamics taking place in the pentacene topmost layers, while charge transfer at the pentacene/C₆₀ and C₆₀/silver interfaces can be neglected. In fact, XAS probes only the two topmost layer of the 5 ML film due to the short electron escape depth at the C K-edge. On the other hand, tr-2PPE has already been shown to be insensitive to the underlying layers for film thicknesses larger than 2 ML¹⁷. Before moving to the picosecond XAS measurements, we characterized the energy position and lifetime of the singlet and triplet excited states in the film by performing reference tr-2PPE measurements¹⁷. Complete details can be found in the Supplementary Note 2. The system was excited by a visible pump pulse ($h\nu = 2.4$ eV) and ionized by a time-delayed ultraviolet probe pulse ($h\nu = 4.8$ eV). With respect to previously published measurements performed with optical pump at 2.15 eV, *i.e.* resonant at the ground state (S₀) to the first excited singlet state (S₁) transition, the 2.4 eV pump photon promotes the electrons from the HOMO to the third singlet excited state (S₃) and from here a fast transition to lower excited singlet states (S₂, S₁) can occur. A similar behaviour has been reported on tetracene thick films²⁵. After the relaxation to S₁, the singlet fission into two triplet excitons (T₁) is energetically favourable. The analysis of the tr-2PPE measurements is reported in Supplementary Fig. 2 for a 2 ML pentacene film on C₆₀/Ag (111). We observe the pump-induced population of a short-lived state (<330 fs, *i.e.* below our temporal resolution) that we attribute to S₃ and of a long-lived (100 ps timescale) state assigned to T₁, providing a picture that is analogous to the case of pentacene/C₆₀ on Au(111)¹⁷.

Time-resolved X-ray absorption. We then performed picosecond carbon K-edge XAS on a 5 ML pentacene film on C₆₀/Ag (111). We excited the sample with 2.4 eV optical pump as in the tr-2PPE and we employed X-ray pulses from Elettra synchrotron as a probe. Details on the experimental set-up can be found in the Methods section and in *ref.* 26. Figure 1 shows the pump-probe scheme at a specific X-ray energy and pump-probe delay. The XAS signal has been recorded by collecting carbon KVV Auger electrons in the first few nanoseconds after the pump excitation (excited or pumped sample) and again after 864 ns, *i.e.* from the unexcited or unpumped sample in the same acquisition temporal frame (green dashed box). This stroboscopic acquisition ensures a proper normalization of the data, hence compensating the X-ray pulse intensity variations due to decay and refilling of the X-ray probe beam in the storage ring. A XAS spectrum is measured at each pump-probe step delay by varying the incoming photon energy via the beamline monochromator. The pump-probe delay is electronically shifted in 50 ps steps. We employed two special operating modes of the synchrotron to obtain 1.157 MHz X-ray pulses, *i.e.* the hybrid and the single bunch filling. In the hybrid mode, the multibunch ring structure (2 ns evenly spaced bunches, 310 mA total current) presents a dark gap of 150 ns where a single X-ray pulse (of about 3 mA, 120 ps) is placed. In the single bunch,

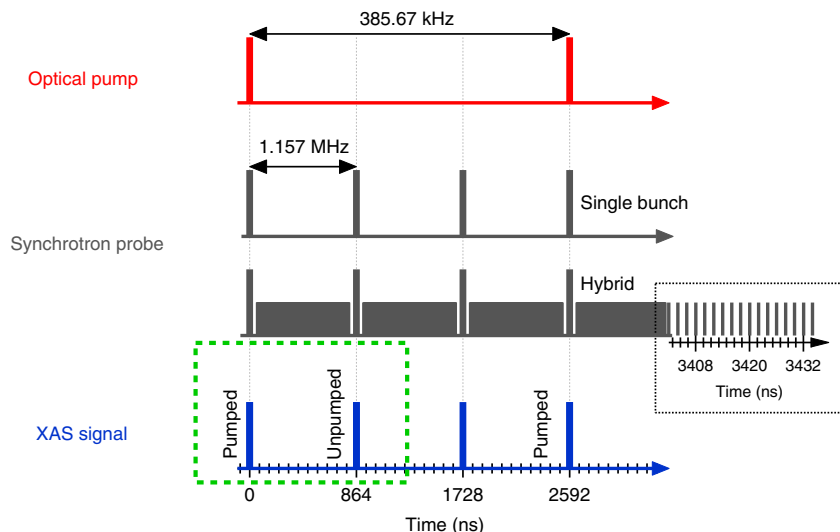


Fig. 1 Scheme of the pump-probe set-up. Temporal distribution of laser (red) and synchrotron (grey) pulses and of the detected X-ray absorption (XAS) signal (blue). The green dashed box indicates the standard acquisition frame

only one X-ray pulse (of about 3 mA, 60 ps) per revolution is delivered to the sample. While the hybrid mode does not affect the normal operation of the synchrotron (in terms of beam energy, current and lifetime), the single bunch mode is run only on request few days per year because the low flux is incompatible with the working conditions of most beamlines at the facility. Of course, for the tr-XAS measurements, the single bunch mode operation has the advantage of a significantly reduced damage due to the lower X-ray photon flux (factor of ~ 0.01) at the sample.

Figure 2 shows the pumped (P, red) and the unpumped (U, blue) carbon K-edge XAS spectra acquired on 5 ML pentacene at the temporal overlap between pump and probe pulses. An expanded photon energy range of the C K-edge XAS on the film comprising the first LUMO and LUMO + 1 transitions is shown in the inset of Fig. 2. We observe a pump-induced intensity increase around 282.5 eV as evidenced by the transient change (P-U/U) in the lower panel of Fig. 2. The absorption intensity in the LUMO region decreases correspondingly, as reported in Supplementary Note 3. Considering that the highest achievable temporal resolution is set to 120 ps by the synchrotron X-ray pulse width and that in tr-2PPE measurements T_1 is the only contribution at delay times longer than a hundred picoseconds, we attribute the pump-induced features in the XAS spectra to T_1 . For what concerns the singlet excited states (S_1 , S_2 , S_3) and the multiexciton (ME), their shorter lifetimes require much shorter X-ray pulses (< 100 fs) to probe them. As a consequence, we can attribute the (optically pumped) XAS state at 282.5 eV to C K-edge transitions originating from pentacene molecules in the triplet excited state. The weak intensity of the measured T_1 can be explained by considering that the pump fluence employed in the experiment yields $\sim 1.3 \times 10^{19}$ excitations cm^{-3} . As each singlet originates two triplets and assuming that all excitations undergo singlet fission and that there are about 10^{21} molecules cm^{-3} , we estimate only 1–2% of the probed molecules to be in the excited state.

Figure 3 shows the behaviour of the integrated transient absorption intensity in the region between 282.3 and 282.8 eV as a function of the pump-probe delay. The two traces have been acquired in hybrid and single bunch synchrotron operation modes. Data acquired in hybrid mode are partly affected by X-ray induced radiation damage due to the higher photon flux, as mentioned above. The corresponding modifications of the carbon

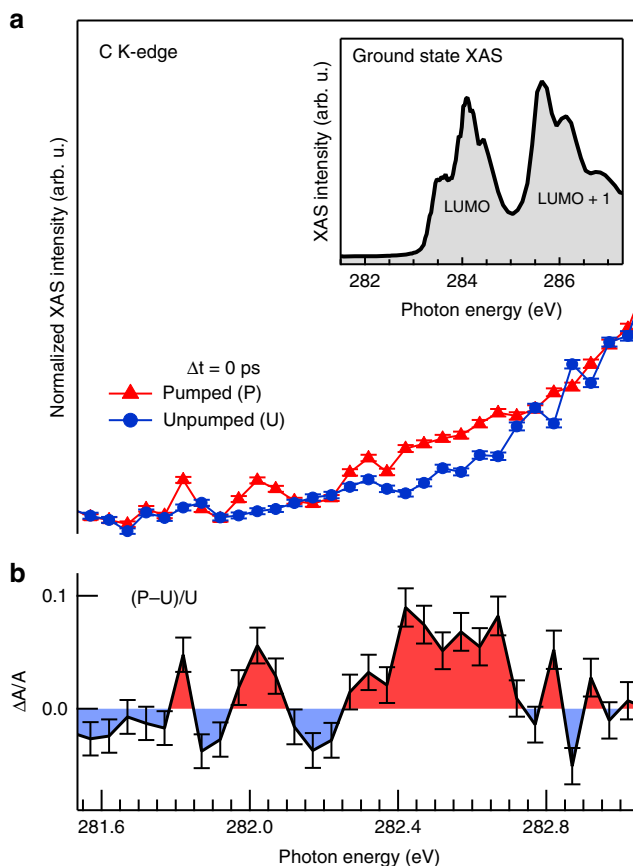


Fig. 2 Pump-probe X-ray absorption on pentacene. **a** Pre-edge region of the pentacene carbon K-edge X-ray absorption spectrum (XAS) with (red) and without (blue) the optical pump at time zero. In the inset an expanded view of the spectra up to the pentacene LUMO + 1 is reported. **b** Transient absorption calculated as ratio (pumped–unpumped)/unpumped. We observe intensity enhancement at about 282.5 eV. Error bars represent one standard deviation

K-edge XAS have been characterized in detail in order to single out the dynamical effects (molecular excitation) from the kinetic ones (molecular decomposition), see Supplementary Note 4. The pink curve in Fig. 3 has been measured by reducing the

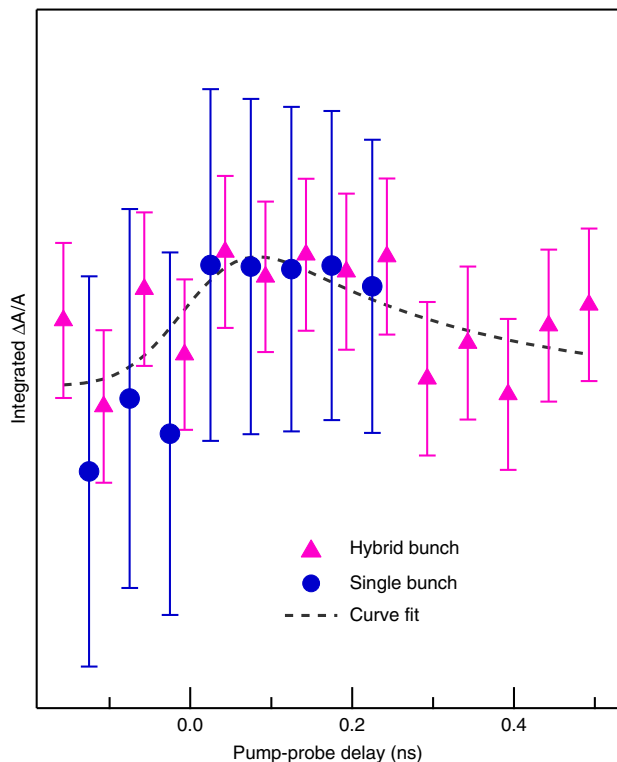


Fig. 3 Transient absorption (integrated $\Delta A/A$) as a function of pump-probe delay. Two datasets are reported, acquired with two different synchrotron operating modes: hybrid (pink) and single bunch (blue). Error bars represent one standard deviation. The hybrid mode data have been fitted by an exponential decay convoluted with a Gaussian (dashed line)

acquisition time to 2 h per delay point, in order to have a compromise between damage effects and signal-to-noise ratio. The hybrid mode data of Fig. 3 have been fitted by the convolution of an exponential decay and a Gaussian function (dashed line). The Gaussian width has been fixed at 120 ps FWHM, the estimated X-ray pulse width. The best fit yields a lifetime of 0.3 ± 0.2 ns. A step at time zero is better visible in the single bunch measurement (blue) in which the X-ray pulse width is halved (about 60 ps). This measurement is also damage free, the drawback being the reduced accumulated data points for each delay step since data collection had to be restricted to a maximum of 20 min. This is due to a shorter lifetime of the electron bunch in the storage ring in such configuration, yielding larger errors and limiting the accessible delay range. The experimentally determined lifetime is well in agreement with previously reported triplet decay time constants in pentacene multilayers measured via tr-2PPE. Chan et al. reported lifetimes ranging between 250 and 400 ps for 2 and 10 ML films, respectively¹⁷. Other transient absorption studies reported 5 ns triplet lifetimes in polycrystalline pentacene films²⁷, but it has been shown in a similar molecule that film morphology plays a crucial role in determining the decay dynamics²⁸. In our case, considering the low diffusion rate along the molecular *c*-axis (10^{-6} cm² s⁻¹)²⁹ and using Fick's law for determining the diffusion length as in ref. 30, it requires ~ 100 ns for the exciton generated in the topmost layers to move 5 nm and reach the interface with C₆₀. This consideration excludes the transfer to C₆₀ from being the preferential decay channel, while it is in agreement with refs. 16,17 on a relaxation process dominated by exciton trapping.

Ab initio calculations. In order to support the experimental identification of T₁ in the transient XAS, we performed ab initio

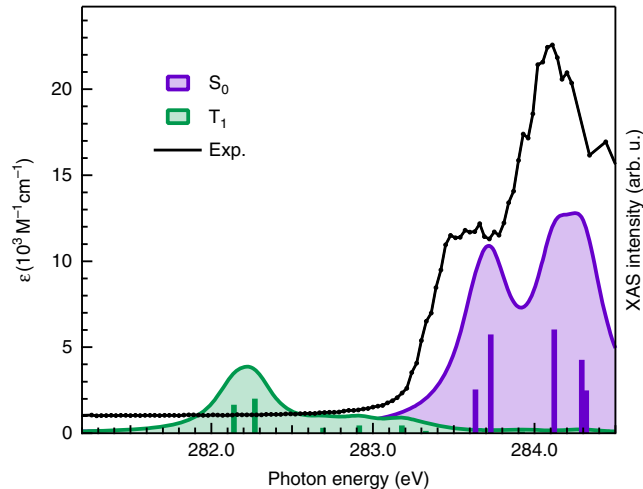


Fig. 4 Calculated X-ray absorption spectra. Ground state (S₀) and triplet excited state (T₁) spectra of a single pentacene molecule are shown. Calculations were performed by implementing a core-valence separation (CVS) scheme within the resolution of identity (RI-) second-order coupled-cluster (CC2) approximation and utilizing the aug-cc-pVTZ basis set. Computed spectra were shifted by -3.2 eV to be aligned to the experimental unpumped spectrum (black line). The S₀ spectrum was computed at the Franck-Condon geometry (RI-CC2/cc-pVTZ optimized), whereas the T₁ spectrum was computed at the relaxed T₁ geometry obtained by the second-order algebraic diagrammatic construction ADC(2) level with the cc-pVTZ basis set

calculations of the core-absorption spectra of both the ground state and the triplet excited state. Figure 4 shows the simulated spectra of the ground state, S₀, and of the T₁ valence excited state at the RI-CC2/aug-cc-pVTZ level of theory. Of the coupled-cluster hierarchy of wave-function methods, the (RI-)CC2 model is the lowest scaling member that is capable of describing electron correlation. Correlation effects are included consistently through second-order perturbation theory. Formally, it has the same computational scaling as second-order Møller-Plesset perturbation theory (MP2), but it is iterative and allows the treatment of excited states. It is also considered superior to time-dependent density functional theory (TDDFT) in terms of accuracy, in particular for the description of triplet excited states^{31,32}. The S₀ spectrum in Fig. 4 was computed at the S₀ minimum, and the T₁ spectrum at the minimum of the T₁ excited state. The T₁ core-excited band was located at around 1.5 eV from the first peak of the LUMO band (NB: the two spectra shown do not take into account the relative populations of ground and T₁ states, experimentally estimated in 98% and 2%, respectively). The computed X-ray absorption spectra of the two states, shown in Fig. 4 with the experimental ground-state spectrum, were both shifted by -3.2 eV. The value of the shift was chosen in order to align the computed ground-state X-ray absorption spectrum to the experimental one. After re-alignment, the RI-CC2 calculations qualitatively support the results of the experimental measurements.

Discussion

In summary, we have shown that time-resolved X-ray absorption spectroscopy at synchrotrons can be used to measure the dynamics of triplet excited states with chemical selectivity. We characterized a 5 ML film of pentacene, the archetypal SF molecule, by means of picosecond carbon K-edge XAS. We experimentally identified in the XAS spectrum of optically excited organic molecules the transitions associated with the fraction of

molecules in the triplet state. Our assignments are theoretically supported by a novel approach in the state-of-the-art calculations. In this work, we established experimental and theoretical protocols for characterizing the long-lived exciton dynamics in SF chromophores with chemical selectivity, which represents a notable advantage over laser-based techniques, such as 2PPE and transient absorption, for the characterization of heterojunctions and multicomponent architectures. Picosecond XAS will provide valuable information about the triplet exciton dynamics in complex structures, therefore helping to achieve a better understanding of the electronic properties of SF chromophores and therefore a better design of SF sensitized solar devices.

Methods

Sample preparation. The organic films have been grown in situ in the same UHV chamber in which all the measurements have been performed (ANCHOR-SUNDYN endstation of the ALOISA beamline at the Elettra synchrotron²⁶). We employed an Ag(111) single crystal as substrate, which was cleaned by repeated Ar⁺ ion sputtering and annealing cycles. A C₆₀ (Sigma Aldrich, 99.9% purity) multilayer was grown on the sample by evaporation from a Knudsen cell ($T_{\text{cell}} = 375$ °C). Subsequently the sample was annealed to 350 °C to obtain a C₆₀ monolayer from the multilayer desorption. The sample quality was monitored by C K-edge XAS. Finally, pentacene layers (Sigma Aldrich, 99.99% purity) were evaporated on the C₆₀ buffer layer from a Knudsen cell ($T_{\text{cell}} = 200$ °C). The calibration of the evaporation rate is detailed in the Supplementary Note 1.

Picosecond carbon K-edge XAS measurements. All measurements have been performed at the ANCHOR-SUNDYN endstation. As a pump, the second harmonic of the Yb-doped Yttrium aluminium garnet (Yb:YAG) fibre laser (Tangerine HP, Amplitude Systèmes) was used. The photon energy was 2.4 eV. Laser and synchrotron beams enter the experimental chamber at 27° and 62° with respect to the surface normal in the measurement geometry. To maximize the overlap with the X-ray spot, we used two cylindrical lenses on the pump beam to achieve an elliptical 0.5×0.25 mm² spot on the sample. The spatial overlap was checked with a YAG crystal mounted on the sample holder, while the temporal overlap was determined by measuring optical pump-induced vacuum space charge effects on the Ag 3d core level lines²⁶. The C K-edge XAS spectra were measured by collecting carbon KVV Auger electrons through a hemispheric electron analyser (PSP Resolve 120), which was set to a kinetic energy of 257 eV with a pass energy of 100 eV. The angle between the analyser and surface normal was 27°. The laser was operated at 385.67 kHz in order to have a pumped and an unpumped synchrotron pulse in each acquisition temporal frame, as depicted in Fig. 1. The measured XAS spectra have been subsequently normalized with the clean sample spectra in order to correct for the beamline transmission. We used a fluence of about 130 μJ cm⁻² to achieve a pump photon density similar to that used for tr-2PPE measurements.

Theory. The ground-state geometry of one single pentacene molecule was optimized at the second-order coupled-cluster level using the resolution of identity approximation (RI-CC2)^{33–35} method and Dunning's cc-pVTZ basis set³⁶, with optimized auxiliary basis sets from ref. 37. The geometry of the valence T₁ state was optimized using the second-order algebraic diagrammatic construction (ADC(2)) approach³⁸, employing the RI approximation³⁹ and the cc-pVTZ basis set. To calculate the XAS spectra of both the ground-state S₀ and the triplet excited state T₁, a core-valence separation (CVS)^{40,41} scheme was implemented, where the core-electron were kept frozen during the wave-function optimization, whereas only excitations involving at least one core orbital were allowed during the solution of the eigenvalue equations. XAS calculations were performed for three different basis set combinations^{42,43}: aug-cc-pVDZ on all atoms, aug-cc-pVTZ on the carbon atoms and aug-cc-pVDZ on the H atoms, and aug-cc-pVTZ on all atoms. The calculations in the different basis sets yielded similar spectral profiles, yet with different absolute shifts (in between 3.2 and 4 eV) from the experimental data, and with the aug-cc-pVTZ basis showing, as expected, the smaller absolute shift. The ground-state excitation energies and transition strengths were obtained within RI-CC2 linear response^{44,45}. The triplet state core-absorption transition strengths were computed as strengths between the valence excited state T₁ and various core-excited states of triplet symmetry^{46,47}. To this end, we extended the implementation of intensities for T₁ → T_n transitions of Pabst and Köhn^{46,48,49} to the case where T_n is a core-excited state. All calculations were performed using the TURBOMOLE package⁵⁰. For the calculations of core spectra, a local version of the ricc2 module was employed. The spectra were simulated by convolution with a Lorentzian broadening function of the computed excitation energies and transition strengths. A value of 1600 cm⁻¹ (0.2 eV) was used for the broadening parameter⁵¹.

Data availability

The data that support the findings of this study are available from the corresponding author on request.

Code availability

The computational methodologies implemented and utilized in this study are available in the TURBOMOLE package⁵⁰, see <http://www.turbomole-gmbh.com/> for additional information on code availability.

Received: 12 December 2018 Accepted: 29 April 2019

Published online: 18 June 2019

References

1. Trupke, T., Green, M. A. & Würfel, P. Improving solar cell efficiencies by down-conversion of high-energy photons. *J. Appl. Phys.* **92**, 1668–1674 (2002).
2. Green, M. A. & Bremner, S. P. Energy conversion approaches and materials for high-efficiency photovoltaics. *Nat. Mater.* **16**, 23–34 (2016).
3. de la Mora, M. B., Amelines-Sarria, O., Monroy, B. M., Hernández-Pérez, C. D. & Lugo, J. E. Materials for downconversion in solar cells: perspectives and challenges. *Sol. Energy Mater. Sol. Cells* **165**, 59–71 (2017).
4. Hanna, M. C. & Nozik, A. J. Solar conversion efficiency of photovoltaic and photoelectrolysis cells with carrier multiplication absorbers. *J. Appl. Phys.* **100**, 074510 (2006).
5. Zirlmeier, J. et al. Singlet fission in pentacene dimers. *Proc. Natl Acad. Sci. USA* **112**, 5325–5330 (2015).
6. Sanders, S. N. et al. Intramolecular singlet fission in oligoacene heterodimers. *Angew. Chem.* **128**, 3434–3438 (2016).
7. Lukman, S. et al. Tuneable singlet exciton fission and triplet-triplet annihilation in an orthogonal pentacene dimer. *Adv. Funct. Mater.* **25**, 5452–5461 (2015).
8. Korovina, N. V. et al. Singlet fission in a covalently linked cofacial alkynyltetracene dimer. *J. Am. Chem. Soc.* **138**, 617–627 (2016).
9. Zimmerman, P. M., Bell, F., Casanova, D. & Head-Gordon, M. Mechanism for singlet fission in pentacene and tetracene: from single exciton to two triplets. *J. Am. Chem. Soc.* **133**, 19944–19952 (2011).
10. Busby, E. et al. A design strategy for intramolecular singlet fission mediated by charge-transfer states in donor-acceptor organic materials. *Nat. Mater.* **14**, 426–433 (2015).
11. Liang, Y. et al. For the bright future-bulk heterojunction polymer solar cells with power conversion efficiency of 7.4%. *Adv. Mater.* **22**, E135–E138 (2010).
12. Kasai, Y., Tamai, Y., Ohkita, H., Bente, H. & Ito, S. Ultrafast singlet fission in a push-pull low-bandgap polymer film. *J. Am. Chem. Soc.* **137**, 15980–15983 (2015).
13. Ponseca, C. S., Chábera, P., Uhlrig, J., Persson, P. & Sundström, V. Ultrafast electron dynamics in solar energy conversion. *Chem. Rev.* **117**, 10940–11024 (2017).
14. Congreve, D. N. et al. External quantum efficiency above 100% in a singlet-exciton-fission-based organic photovoltaic cell. *Science* **340**, 334–337 (2013).
15. Yost, S. R. et al. A transferable model for singlet-fission kinetics. *Nat. Chem.* **6**, 492–497 (2014).
16. Marciniak, H. et al. Ultrafast exciton relaxation in microcrystalline pentacene films. *Phys. Rev. Lett.* **99**, 176402 (2007).
17. Chan, W.-L. et al. Observing the multiexciton state in singlet fission and ensuing ultrafast multielectron transfer. *Science* **334**, 1541–1545 (2011).
18. Van Kuiken, B. E. et al. Picosecond sulfur K-edge X-ray absorption spectroscopy with applications to excited state proton transfer. *Struct. Dyn.* **4**, 044021 (2017).
19. Bhattacharjee, A., Pemmaraju, C. Das, Schnorr, K., Attar, A. R. & Leone, S. R. Ultrafast intersystem crossing in acetylacetone via femtosecond X-ray transient absorption at the carbon K-edge. *J. Am. Chem. Soc.* **139**, 16576–16583 (2017).
20. Milne, C. J., Penfold, T. J. & Chergui, M. Recent experimental and theoretical developments in time-resolved X-ray spectroscopies. *Coord. Chem. Rev.* **277**, 44–68 (2014).
21. Chen, L. X., Zhang, X. & Shelby, M. L. Recent advances on ultrafast X-ray spectroscopy in the chemical sciences. *Chem. Sci.* **5**, 4136–4152 (2014).
22. Chergui, M. Time-resolved X-ray spectroscopies of chemical systems: new perspectives. *Struct. Dyn.* **3**, 031001 (2016).
23. Nilsson, A. et al. Catalysis in real time using X-ray lasers. *Chem. Phys. Lett.* **675**, 145–173 (2017).
24. Dougherty, D. B., Jin, W., Cullen, W. G., Reutt-Robey, J. E. & Robey, S. W. Striped domains at the pentacene:C60 interface. *Appl. Phys. Lett.* **94**, 023103 (2009).
25. Chan, W.-L., Ligges, M. & Zhu, X.-Y. The energy barrier in singlet fission can be overcome through coherent coupling and entropic gain. *Nat. Chem.* **4**, 840–845 (2012).
26. Costantini, R. et al. ANCHOR-SUNDYN: a novel endstation for time resolved spectroscopy at the ALOISA beamline. *J. Electron Spectros. Relat. Phenom.* **229**, 7–12 (2018).

27. Rao, A. et al. Exciton fission and charge generation via triplet excitons in pentacene/C60 bilayers. *J. Am. Chem. Soc.* **132**, 12698–12703 (2010).
28. Burdett, J. J., Müller, A. M., Gosztola, D. & Bardeen, C. J. Excited state dynamics in solid and monomeric tetracene: the roles of superradiance and exciton fission. *J. Chem. Phys.* **133**, 144506 (2010).
29. Smith, M. B. & Michl, J. Singlet fission. *Chem. Rev.* **110**, 6891–6936 (2010).
30. Akselrod, G. M. et al. Visualization of exciton transport in ordered and disordered molecular solids. *Nat. Commun.* **5**, 3646 (2014).
31. Grotjahn, R., Maier, T. M., Michl, J. & Kaupp, M. Development of a TDDFT-based protocol with local hybrid functionals for the screening of potential singlet fission chromophores. *J. Chem. Theory Comput.* **13**, 4984–4996 (2017).
32. Schreiber, M., Silva-Junior, M. R., Sauer, S. P. A. & Thiel, W. Benchmarks for electronically excited states: CASPT2, CC2, CCSD, and CC3. *J. Chem. Phys.* **128**, 134110 (2008).
33. Christiansen, O., Koch, H. & Jørgensen, P. The second-order approximate coupled cluster singles and doubles model CC2. *Chem. Phys. Lett.* **243**, 409–418 (1995).
34. Hättig, C. & Weigend, F. CC2 excitation energy calculations on large molecules using the resolution of the identity approximation. *J. Chem. Phys.* **113**, 5154 (2000).
35. Hättig, C. Geometry optimizations with the coupled-cluster model CC2 using the resolution-of-the-identity approximation. *J. Chem. Phys.* **118**, 7751–7761 (2003).
36. Dunning, T. H. Gaussian basis sets for use in correlated molecular calculations. I. The atoms boron through neon and hydrogen. *J. Chem. Phys.* **90**, 1007–1023 (1989).
37. Weigend, F., Köhn, A. & Hättig, C. Efficient use of the correlation consistent basis sets in resolution of the identity MP2 calculations. *J. Chem. Phys.* **116**, 3175–3183 (2002).
38. Schirmer, J. Beyond the random-phase approximation: a new approximation scheme for the polarization propagator. *Phys. Rev. A* **26**, 2395–2416 (1982).
39. Hättig, C. Structure optimizations for excited states with correlated second-order methods: CC2 and ADC(2). *Adv. Quantum Chem.* **50**, 37–60 (2005).
40. Cederbaum, L. S., Domcke, W. & Schirmer, J. Many-body theory of core holes. *Phys. Rev. A* **22**, 206–222 (1980).
41. Coriani, S. & Koch, H. Communication: X-ray absorption spectra and core-ionization potentials within a core-valence separated coupled cluster framework. *J. Chem. Phys.* **143**, 181103 (2015).
42. Woon, D. E. & Dunning, T. H. Gaussian basis sets for use in correlated molecular calculations. V. Core-valence basis sets for boron through neon. *J. Chem. Phys.* **103**, 4572–4585 (1995).
43. Kendall, R. A., Dunning, T. H. & Harrison, R. J. Electron affinities of the first-row atoms revisited. Systematic basis sets and wave functions. *J. Chem. Phys.* **96**, 6796–6806 (1992).
44. Hättig, C. & Hald, K. Implementation of RI-CC2 triplet excitation energies with an application to trans-azobenzene. *Phys. Chem. Chem. Phys.* **4**, 2111–2118 (2002).
45. Hättig, C. & Köhn, A. Transition moments and excited-state first-order properties in the coupled-cluster model CC2 using the resolution-of-the-identity approximation. *J. Chem. Phys.* **117**, 6939–6951 (2002).
46. Pabst, M. & Köhn, A. Implementation of transition moments between excited states in the approximate coupled-cluster singles and doubles model. *J. Chem. Phys.* **129**, 214101 (2008).
47. Hättig, C., Köhn, A. & Hald, K. First-order properties for triplet excited states in the approximated coupled cluster model CC2 using an explicitly spin coupled basis. *J. Chem. Phys.* **116**, 5401–5410 (2002).
48. Pabst, M., Lunkenheimer, B. & Köhn, A. The triplet excimer of naphthalene: a model system for triplet-triplet interactions and its spectral properties. *J. Phys. Chem. C* **115**, 8335–8344 (2011).
49. Pabst, M., Sundholm, D. & Köhn, A. Ab initio studies of triplet-state properties for organic semiconductor molecules. *J. Phys. Chem. C* **116**, 15203–15217 (2012).
50. Furcher, F. et al. Turbomole. *Wiley Interdiscip. Rev. Comput. Mol. Sci.* **4**, 91–100 (2014).
51. Fratesi, G., Lanzilotto, V., Floreano, L. & Brivio, G. P. Azimuthal dichroism in near-edge X-ray absorption fine structure spectra of planar molecules. *J. Phys. Chem. C* **117**, 6632–6638 (2013).

Acknowledgements

M.D.A. and R.C. acknowledge support from the SIR grant SUNDYN [Nr RBSI14G7TL, CUP B82I15000910001] of the Italian Ministry of Education Universities and Research MIUR. The experimental work has been supported by EUROPOL MIUR Progetti Internazionali. R.F. and S.C. acknowledge financial support from DTU Chemistry and from the Independent Research Fund Denmark - DFF-Forskningsprojekt2 grant no. 7014-00258B. The Marie Skłodowska-Curie European Training Network “COSINE—Computational Spectroscopy In Natural sciences and Engineering” is also acknowledged. C.H. acknowledges financial support by the Deutsche Forschungsgemeinschaft (DFG) through grant no. Ha-2588/7-2.

Author contributions

R.C. and M.D.A. designed the experiment. R.C., A.C., L.F., A.V., A.M. and M.D.A. performed the experiments and analysed the data. C.H. implemented the CVS-RI-CC2 methodology for (excited-state) core spectra. R.F., C.H. and S.C. performed the theoretical calculations. All the authors discussed the results and commented on the manuscript.

Additional information

Supplementary information accompanies this paper at <https://doi.org/10.1038/s42005-019-0157-1>.

Competing interests: The authors declare no competing interests.

Reprints and permission information is available online at <http://npg.nature.com/reprintsandpermissions/>

Publisher's note: Springer Nature remains neutral with regard to jurisdictional claims in published maps and institutional affiliations.



Open Access This article is licensed under a Creative Commons Attribution 4.0 International License, which permits use, sharing, adaptation, distribution and reproduction in any medium or format, as long as you give appropriate credit to the original author(s) and the source, provide a link to the Creative Commons license, and indicate if changes were made. The images or other third party material in this article are included in the article's Creative Commons license, unless indicated otherwise in a credit line to the material. If material is not included in the article's Creative Commons license and your intended use is not permitted by statutory regulation or exceeds the permitted use, you will need to obtain permission directly from the copyright holder. To view a copy of this license, visit <http://creativecommons.org/licenses/by/4.0/>.

© The Author(s) 2019